Customer-side SCADA-assisted Large Battery Operation Optimization for Distribution Feeder Peak Load Shaving

Zach Taylor, *Student Member, IEEE*, Hossein Akhavan-Hejazi, *Member, IEEE*, Ed Cortez, Lilliana Alvarez, *Professional Member, IEEE*, Sadrul Ula, *Senior Member, IEEE*, Matthew Barth, *Fellow, IEEE*, and Hamed Mohsenian-Rad, *Senior Member, IEEE*

***Abstract*—Built upon real-world SCADA and other measurements of a featured utility-scale testbed, this paper addresses the participation of customer side battery energy storage in providing peak load shaving at a 12.47 kV distribution feeder. A stochastic optimization-based battery operation framework is developed that enables feeder load peak shaving under offline (day-ahead) as well as online (close-to-real-time) control settings. Both designs work through establishing a secured communications line to the utility's feeder-level SCADA system. Multiple field experiments are conducted, including a full day test with complete control of a 1 MWh / 200 kW battery system, as well as various numerical assessments based upon one year of real feeder data.**

***Keywords*: Feeder-level peak-load shaving, utility-scale testbed, battery systems, stochastic optimization, energy storage, substation, distributed energy resources, communications.**

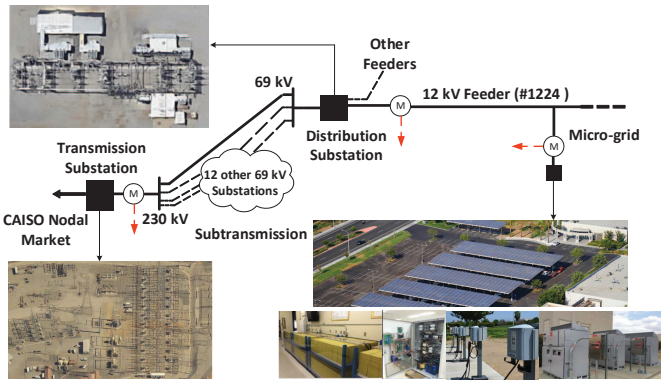

Fig. 1. A wide view of the overall utility-scale test system in this study.

I. Introduction

The principles of utilizing customer side battery resources for distribution feeder peak load reduction are simple [1], [2]; yet there are several technical challenges that need to be addressed in practice. For example, any arrangement for customer-side battery resources to respond to changes in feeder load would require communications between the customer and the utility's feeder-level supervisory control and data acquisition (SCADA) system. Some of these issues are gradually being addressed, e.g., in recent regulatory efforts such as in [3]. However, additional studies and access to real-world test data are needed to understand how customers can provide feeder-level utility-scale services. Accordingly, the goal of this paper is to *identify, explain, and characterize the challenges in utilizing customer-side battery resources to conduct distribution feeder peak load reduction.* The analysis in this paper is built upon a utility-scale testbed developed through a university-utility collaboration in Riverside, CA.

A. Utility-Scale Test Setup

The test set up in this project has two main components: a micro-gridin a commercial building; and a communications platform between the utility SCADA system and the microgrid. Several distributed energy resources (DERs) are installed at the microgrid, including a battery system with 1 MWh energy and 200 kW power ratings, three solar arrays with a total of 460 kW nominal capacity, and several level-2 electric vehicle chargers. The building is served by a 12.47 kV feeder, number #1224, on Riverside Public Utilities (RPU)'s 69 kV Hunter Station. The test setup is shown in Fig. 1. This figure also shows how the Hunter substation is located with respect to the rest of the sub-transmission, and transmission systems. Additional details about this testbed are discussed in [4]–[8].

As a key feature of this test platform, the microgrid battery controller is granted access to the utility's SCADA system to remotely read the feeder's active and reactive power load data in a *minute-by-minute* resolution. This is facilitated through establishing a secured communications line[1].

B. Contributions

The contributions in this paper are summarized as follows:

- To the best of our knowledge, this is the first study to develop and test a real-world utility-scale optimization-based customer-side battery operation mechanism in order to perform peak-shaving at a distribution feeder.
- A battery scheduling framework based on stochastic optimization is developed that utilizes various measurements, accounts for feeder load uncertainties in offline (day-ahead) and online (close-to-real-time) control settings, and addresses various design objectives and constraints.
- Multiple real-world field experiments, including a full-day full-scale field test, are conducted and the results are analyzed. Also, one year of real-world feeder data is used to extend the experiments and to report a variety of lessons learned, such as the impact of load estimation

Z. Taylor, H. Hejazi, and H. Mohsenian-Rad are with the Department of Electrical Engineering, University of California, Riverside, CA, USA. E. Cortez and L. Alvarez are with Riverside Public Utilities, Riverside, CA, USA. S. Ula and M. Barth are with the Center for Environmental Research & Technology, University of California, Riverside, CA, USA. This work was supported by RPU EI Grant 14-2853, NSF Grant 1253516, DoE Grant EE 0008001, and also by Winston Chung Global Energy Center. The corresponding author is H. Mohsenian-Rad, email: hamed@ee.ucr.edu.

[1]The authors would like to thank Alan Woodcock, Alan Lee, Ed Sponsler, and Alex Vu for their help in establishing the secure communications line.

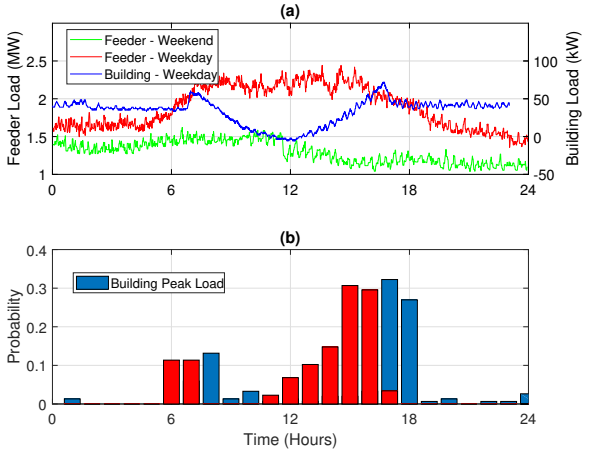

Fig. 2. Comparison of the load profiles at the feeder and at the building; (a) the sample feeder profile on a weekend and the sample feeder and building load profiles on a weekday; (b) the distributions of the feeder and building's peak load hours during the utility's Winter season.

errors, battery charge estimation errors, battery round-trip efficiency, and the trade-offs and conflicts across system-level, feeder-level, and customer-level objectives.

C. Related Work

The related literature can be classified into several groups. First, there are papers that are solely based on simulations, as opposed to on real-world data and experiments as in this paper. They address different goals for energy storage operation, such as peak load shaving [9]–[11] or voltage control [12]. Among them, only [10] is related to customer-side energy storage operation, where the focus is on plug-in electric vehicles.

Second, there are energy storage operation studies that incorporate real-world measurements into computer simulations, such as in [13]–[15]. The study in [13] is about building load shifting for billing purposes using real-world building load data, as opposed to feeder-load shaving as a service to utility. The studies in [14], [15] operate storage as a grid asset, as opposed to a customer asset. They do not address the feeder load uncertainty either. The studies in this second group do not involve any field experiment; thus, they too may not fully replicate the practical observations in real-world experiments.

Third, there are studies, e.g. in [16]–[18], which include field experiments to utilize energy storage resources for feeder-level applications. However, to the best of our knowledge, all such studies focus on *utility-owned* energy storage resources, as opposed to customer-side resources as in this paper. In this regard, they essentially address a different direction of research compared to this manuscript. For example, they do not address the utility-coordinated DER operation, i.e. a DER that is in communication with utility, with customer side considerations and constraints with access to utility's feeder level data. Similarly, they inherently do not face the conflicts of interests between customer side objectives and utility goals.

Compared with the shorter conference version of this work in [19], this paper presents new experimental field tests, more analysis based on real-world feeder data, enhanced framework and formulations, new case studies, and additional discussions.

II. Discovery Analysis of the Feeder Data

We start off, in this section, by seeking to uncover various complications that may exist in the operational conditions across the customer, distribution, and sub-transmission systems. The examination of the available field data, provides evidence and design hints for some key concepts with respect to the operation of the distribution grid with active customers, which shed light on the development of an effective design.

A. Conflict of Feeder-level and Customer-level Requirements

Examples of the feeder daily load profiles are shown in Fig. 2(a) for July 10, a representative week-day, and July 18, a representative weekend. First, we see that the weekday profile has clear peak hours, while the weekend load is fairly flat. Similar trends are observed throughout the SCADA data. Therefore, our focus in this study is on weekdays. Second, we see that the utility feeder peak load often does *not* last long, which means even a relatively small battery system might be able to make a noticeable impact on the feeder peak load.

Fig. 2(a) also shows the *net load* of the building on the same weekday. We see that the peak load hours of the building are *very different* from those of the feeder. This is also confirmed in Fig. 2(b), where the distributions of the peak load hours for the feeder and for the building - without battery operation - are shown during the Winter. The Summer season at this utility is from June to September and the Winter season is from October to May. From Fig. 2(b), it is inferred that, should the customer seek to lower its *own* peak demand, it will *not* necessarily lower the distribution feeder peak load; to the contrary, it could even *increase* the peak. Thus, the demand charges that a utility sets to reduce a customers peak load, do *not* necessarily lead to reducing the peak demand on the distribution feeder. Of course, since the feeder load is the combination of many customer loads, this is not necessarily strange, however it does show that there is potential for conflict and that any schema that is developed in which a customer provides grid services, like feeder peak shaving, must consider these potential conflicts that have impacts on the design.

B. Conflict of Feeder-Level and Utility-wide Requirements

Next, we compare the average daily load of the feeder with the average daily load of the entire sub-transmission system, i.e., the utility as a whole. The comparison is done for the month of February, which is within the utility's Winter season. The results are shown in Fig. 3. We can see that, the peak load hour at the feeder is very different from the peak hour at the utility as a whole. This observation is notable, as it suggests that the system-wide policies for the control and correction of the load profile, such as time-of-use (ToU) pricing, may *not* often help with peak load shaving at this feeder.

Next, we compare the distribution of the daily peak load hour at the feeder, with that of the daily peak price hour in the California ISO day-ahead market. The price data is based on the locational marginal price (LMP) at the transmission-level Vista substation. Note that, the entire RPU sub-transmission system is interconnected with the rest of the California transmission grid, at Vista substation. The results are shown in Fig.

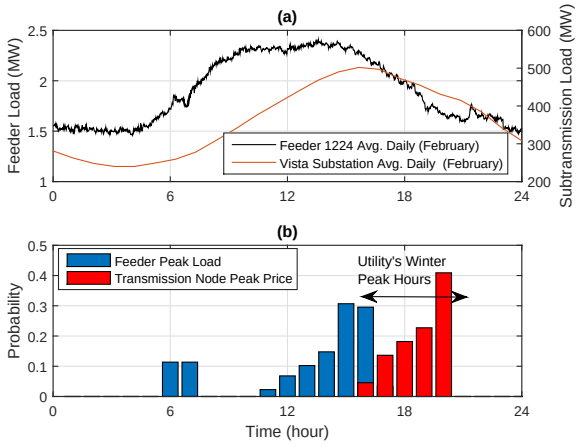

Fig. 3. Comparison of the load profiles at the feeder with those of the sub-transmission system (Vista); (a) the average load profiles of the feeder, and the sub-transmission are shown during an example month of RPU's Winter season, (b) The distributions of peak load hour at the feeder, and peak price hour at the Vista market node are shown during the Winter.

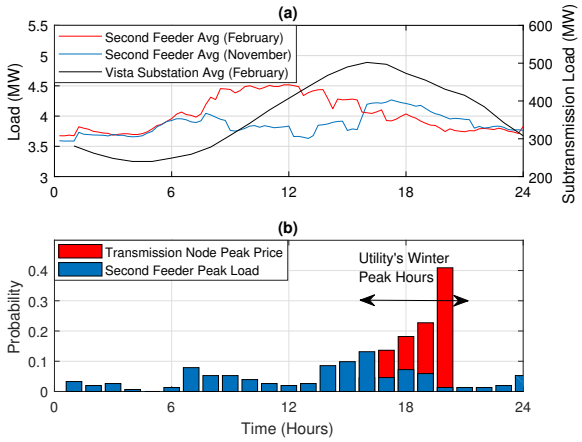

Fig. 4. Comparison of the load profiles at the second feeder with those of the sub-transmission system (Vista); (a) the average load profiles of the feeder, and the sub-transmission are shown during RPU's Winter season; (b) the distributions of peak load hour at the second feeder, and peak price hour at the Vista market node are shown during the Winter.

3(b). We can see that the distribution of the peak price hour based on LMP data generally matches the utility ToU hours. However, this distribution is very different from that of the feeder peak load. While the peak price hour is often between 5:00-9:00 PM, the peak load hour at the feeder is rarely after 4:00 PM, possibly since the feeder serves a commercial area, where the peak load often occurs during business hours.

C. The Need for Localized Solution

The analysis in Sections II-A and II-B, further motivates the goal of our study to conduct peak load reduction at *feeder-level* through a *localized solution*, rather than a customer-level or a utility-wide solution; recall Figs. 2 and 3. It also shows the *conflict* between the best ways to run the battery system as a customer-side financial asset versus the best ways to run the battery to contribute to feeder-level peak load reduction.

We should point out, however, that while the above analysis and observations show *the possibility* that following system-wide policies would not necessarily lead to reducing feeder peak loading condition, we cannot make statements on the generality or severity of such conditions on other feeders. For instance, we analyzed the loading conditions of a second feeder, that is geographically close but is electrically isolated from the Feeder 1224. The analysis was performed on the winter data from October to February. The results are shown in Fig. 4. Here, we can see that for this second feeder, the peak hour conflict with utility peak hours also exist, yet it is not as sever as Feeder 1224. Nevertheless, regardless of the frequency of the feeders that may have conflicts with the utility-wide load pattern, for those feeder that this conditions do exist a localized solution would be effective and necessary.

III. Optimal Battery-Assisted Distribution Feeder Peak Load Reduction

In this section, we present two optimization-based approaches, *offline* and *online*, to operate the 1 MWh / 200 kW battery system at the building, so as to perform feeder peak load shaving. The offline approach is a day-ahead control mechanism. The online approach however uses close-to-real-time access to the data in the utility's SCADA system.

We assume granularity Δ for all charge and discharge schedules of the battery system. Unless stated otherwise, $\Delta = 15$ minutes. Each charge or discharge interval is referred to as one time slot. The charge and discharge schedule at time slot τ is denoted by $x[\tau]$, where $\tau \in \mathcal{T} = [1, \cdots, T]$. Here, $x[\tau]$ takes a *positive* value if we charge the battery and a *negative* value if we discharge the battery. We denote the average feeder load at time slot τ by $l[\tau]$. Note that, $l[\tau]$ is a random variable, whereas $x[\tau]$ is a decision variable. We define $\boldsymbol{l} \triangleq [l[1]; \cdots; l[T]]$ and $\boldsymbol{x} \triangleq [x[1]; \cdots; x[T]]$.

A. Offline Optimization Approach

In the offline approach, the battery controller has access to the feeder-level SCADA data *once per day*, in the evening. Accordingly, the schedule $\boldsymbol{x}$ is decided once at the beginning of each day and such schedule is *not* changed during the day.

1) Objective Function: In the offline approach, we seek to minimize the expected daily feeder peak load, i.e., the expected maximum of the utility feeder load across all the T time slots during the next day. This objective can be formulated as

$$\mathbb{E}\{\max_{\tau \in \mathcal{T}} (l[\tau] + x[\tau])\}, \tag{1}$$

where $\mathbb{E}$ denotes mathematical expectation. The expected value is calculated with respect to the feeder load vector $\boldsymbol{l}$.

The objective in (1) can be interpreted by considering that the feeder peak load is the daily maximum, i.e., the maximum over the time periods $[1, ..., T]$, of the total load which at any given time t, can be disaggregated as the sum of battery output power $x[t]$ that can be controlled, plus the rest of feeder load $l[t]$ that is uncontrollable. Additionally, since $l[t]$ is a random variable, the feeder peak load which is a function of this variable is a random variable as well. Accordingly, we shall minimize the expected value of this random variable.

Even if the probably distribution of random vector $\boldsymbol{l}$ is known, it is still not a straightforward task to use the objective function in (1) in an optimization problem due to the presence

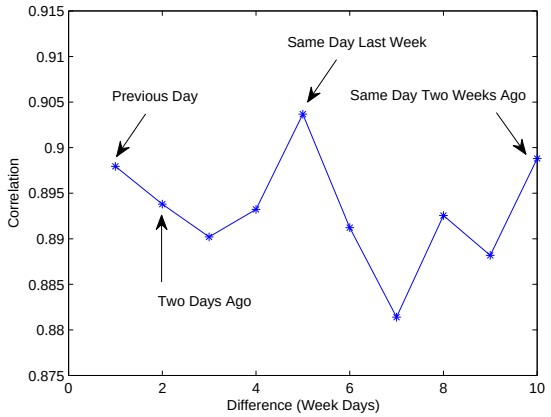

Fig. 5. The correlation of the load on Feeder #1224 on a weekday with the loads on Feeder #1224 on the 10 previous weekdays over the past two weeks.

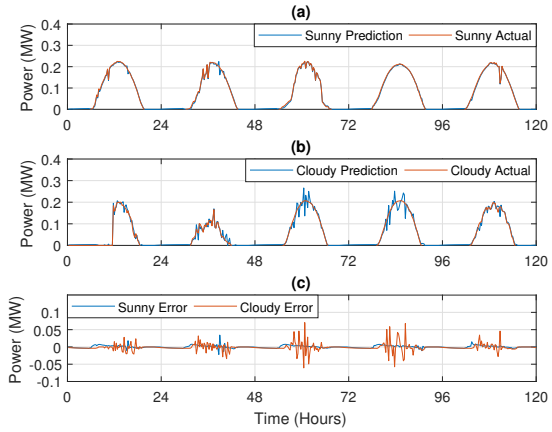

Fig. 6. The results on separate solar generation forecast: (a) Actual and predicted solar output for a sunny week; (b) actual and predicted solar output for a cloudy week; (c) estimation error for both the sunny and cloudy forecasts

of the max function inside the expected value operator. One quick fix is to *approximately* replace (1) with

$$\max_{\tau\in\mathcal{T}} \left(\mathbb{E}\{l[\tau]\} + x[\tau]\right) = \|\mathbb{E}\{\boldsymbol{l}\} + \boldsymbol{x}\|_\infty, \tag{2}$$

where the stochastic nature of the problem is now abstracted into a single expected value of the feeder load vector [20], [21]. Of course, due to Jensen's inequality, the above objective function provides only an *upper bound* for the original objective in (1), c.f. [22, p.77]. Therefore, the optimality gap could potentially be significant, see Section IV-B.

In order to create a more robust model, suppose the randomness in $\boldsymbol{l}$ is modeled using S scenarios, each with a probability γ_s that is weighted according to the correlation of that previous day to the current day (see Fig. 5). We can rewrite (1) as

$$\sum_{s=1}^{S} \gamma_s \|\boldsymbol{l}_s + \boldsymbol{x}\|_\infty. \tag{3}$$

Note that, the above expression is a convex function [22, p.79]. Nevertheless, the difficulty in solving a minimization problem that has (3) as its objective function is to properly choose S as well as γ_s and $\boldsymbol{l}_s$ for each $s = 1, \ldots, S$.

Another challenge is to properly estimate the distribution of $\boldsymbol{l}$ from the historical data. This challenge can be tackled once we can leverage the key data-driven observation that the *cross-correlation* between the daily load profile on one day and those on its prior days is quite high for Feeder #1224, see Fig. 5. The correlation analysis is done on the feeder load time series based on all *weekdays*, see Section II, for one year of real-world load data [23]. We can see that a high correlation, i.e., above 0.88, exists between today's load and the load yesterday, the day before yesterday, and the same day last week. Therefore, it is reasonable to use an *auto regressive moving average* (ARMA) model to estimate the feeder's daily load using data over the past $P = 10$ weekdays [24]:

$$l[\tau] = \sum_{p=1}^{P} a_{p,\tau} l_{-p}[\tau] + e[\tau] \qquad \forall \tau \in \mathcal{T}, \tag{4}$$

where l_{-p} denotes the load at p weekdays *prior* to the present day; $a_{1,\tau}$ to $a_{P,\tau}$ denote the ARMA model coefficients for each weekday in the past P weekdays; and $e[\tau]$ denotes the estimation error at each time slot, which is assumed to have a zero mean and a Gaussian distribution [25], also see [26].

There are different approaches to obtain the coefficients in (4), such as the methods provided in [27], [28]. Here, we select the coefficients by solving the Yule-Walker equations for the seasonal historical data on different days [29]. The coefficients are set lower for older data. From (4), we arrive at a distribution for the random feeder load vector $\boldsymbol{l}$. We can then use this distribution to generate scenarios using a uniform discretization grid, e.g., by using equal weight scenarios that follow the distribution of the intended random variable. Other Monte-Carlo sampling methods, such as sample average approximation (SAA) can also be used, c.f. [30].

With this forecasting method, the impact of DERs on the feeder load is considered *implicitly* in the randomness of the customer load, because the net load is considered as one quantity. This was done for simplicity of the analysis and implementation and also because the penetration of DERs in this real-world testbed is still not too high, despite the fact that it is higher than most typical feeders. Note that, the only major DERs on the understudy real-world feeder are the PVs and batteries that are part of this study itself. Still, the DER deployment at this test feeder, with more than 15% of feeder average peak load, is among the largest across the RPU service territory. For a majority of the feeders, even in larger utilities, e.g. Southern California Edison, the target hosting capacity of DERs is well below 15% [25]. Nevertheless, if the DER penetration level increases, the forecast could be more accurate if the output of solar PV generation is obtained separately.

One can use an ARMA model similar to the one above to separately forecast the PV profile. Such disaggregation approach that relies only on previous PV data works very well in sunny days. An example is shown in Fig 6.

In the presence of bad days with major clouds and rains, an ARMA model does not do well in forecasting PV output on its own. In such a case, one should rather use more advanced solar prediction methods, that use weather, temperature, and cloud data, such as cloud imaging [31]–[33], in order to forecast the solar output. If such advanced forecasting methods are available, they can be integrated into our design framework as

5 well. However, from the practical perspective, the use of such advanced methods to separately forecast solar generation is not in the scope of this paper, as there is no concern at this point or in foreseeable future on the forecast performance degradation (due to extreme DER penetration) on the understudy feeder.

2) Battery Operation Constraints: Several constraints need to be considered to assure proper operation of the battery system. Here, we model the most basic and typical constraints. More details on battery operation constraints is available in [34]. We will also examine some practical aspects with respect to battery system modeling later in Section IV-A.

Let $C[\tau]$ denote the state-of-charge (SoC) at the end of time slot τ. Suppose $\eta^c_{\text{bat}} \leq 1$ and $\eta^d_{\text{bat}} \geq 1$ denote the *charge-* and *discharge-efficiency* parameters of the battery cells, respectively. We can model the changes in SoC as

$$C[\tau]=C[\tau-1]+\Delta t(\eta^c_{\text{bat}}x^c[\tau]-\eta^d_{\text{bat}}x^d[\tau]),\ \forall\tau\in\mathcal{T}, \quad (5)$$

where $x^c[\tau]\geq 0$ and $x^d[\tau]\geq 0$ are the charge and discharge power at battery terminals; $C[0]$ is the *initial SoC* at the start of day. The second term is the energy that is charged into or drawn from the battery at a time slot. The following constraints can capture the relationship between $x[\tau]$, $x^c[\tau]$, and $x^d[\tau]$:

$$\begin{aligned} &x[\tau]=\eta^c_{\text{inv}}x^c[\tau]-\eta^d_{\text{inv}}x^d[\tau] && \forall\tau\in\mathcal{T},\\ &0\leq x^c[\tau]\leq\theta[\tau]x^{\max} && \forall\tau\in\mathcal{T},\\ &0\leq x^d[\tau]\leq(1-\theta[\tau])x^{\max} && \forall\tau\in\mathcal{T}, \end{aligned} \quad (6)$$

where $\theta[\tau]$ is an *auxiliary binary variable* and $x^{\max}$ is the maximum charge and discharge rate of the battery inverters. Accordingly, $\eta^c_{\text{inv}}\geq 1$ and $\eta^d_{\text{inv}}\leq 1$ denote the *charge efficiency* and *discharge efficiency* parameters of the inverter. Since $\theta[\tau]$ takes only 0 or 1, it can force the batteries to be either charging ($\theta=1$) or discharging ($\theta=0$), but not both.

In practice, the SoC for batteries should be kept within certain ranges that assure the health of the battery:

$$C^{\min}\leq C[\tau]\leq C^{max} \quad \forall\tau\in\mathcal{T}, \quad (7)$$

where $0\leq C^{\min}\leq C^{\max}\leq C^{\text{full}}$. For the batteries at our microgrid, $C^{\min}=0.2$, $C^{\max}=0.9$, and $C^{\text{full}}=1$ MWh.

Additionally, we may enforce the following constraint to keep the SoC at the end of each day to always be above a minimum level in order to assure energy availability:

$$C^0\leq C[T], \quad (8)$$

where $C^0\geq C^{\min}$ is a predetermined design parameter. In this paper we use $C^0=C[0]$.

Another constraint is about the charge and discharge rates:

$$-x^{\max}\leq x[\tau]\leq x^{\max} \quad \forall\tau\in\mathcal{T}. \quad (9)$$

For the battery inverters at our microgrid, $x^{\max}=200$ kW.

Finally, one may want to restrict the charging of the batteries to hours other than the utility's system-wide peak-hours. This can be achieved by imposing the following constraints:

$$x[\tau]\leq 0 \quad \forall\tau\in\text{Utility Peak Hours}. \quad (10)$$

B. Online Optimization Approach

In the online approach, the battery controller has *close-to-real-time* access to the utility SCADA system. As in the offline design, an initial schedule is obtained at the beginning of the day, however, the schedule is then updated *at every time slot* as more data becomes available, using a receding horizon optimization approach, c.f. [35]. This allows the optimization to take into account today's load conditions as they develop.

1) Objective Function: Suppose we are at time slot κ, where κ is between 1 to T. At this point in time, we have already implemented schedules $\hat{x}[1],\ldots,\hat{x}[\kappa-1]$, and we know the load values $\hat{l}[1],\ldots,\hat{l}[\kappa-1]$. Next, we want to select schedules $x[\tau]$, where $\tau=\kappa,\ldots,T$. Let $\boldsymbol{l}^\kappa\triangleq[l[\kappa],\ldots,l[T]]$, $\hat{\boldsymbol{l}}^{-\kappa}\triangleq[\hat{l}[1],\ldots,\hat{l}[\kappa-1]]$, $\boldsymbol{x}^\kappa\triangleq[x[\kappa],\ldots,x[T]]$, and $\hat{\boldsymbol{x}}^{-\kappa}\triangleq[\hat{x}[1],\ldots,\hat{x}[\kappa-1]]$. We again minimize the expectation of peak net load, i.e. feeder load plus storage, but subject to the *observations* of $\hat{\boldsymbol{l}}^{-\kappa}$. We can write the objective as

$$\mathbb{E}\{\|\boldsymbol{l}+\boldsymbol{x}\|_\infty|\hat{\boldsymbol{l}}^{-\kappa}\}. \quad (11)$$

Once we separate the random feeder loads and battery decision variables for the remaining horizon versus the already observed values, we can re-write (11) as

$$\begin{aligned} \mathbb{E}\left\{\left\|\begin{bmatrix}\boldsymbol{l}^\kappa\\ \hat{\boldsymbol{l}}^{-\kappa}\end{bmatrix}+\begin{bmatrix}\boldsymbol{x}^\kappa\\ \hat{\boldsymbol{x}}^{-\kappa}\end{bmatrix}\right\|_\infty\middle|\hat{\boldsymbol{l}}^{-\kappa}\right\} \\ =\mathbb{E}\{(\|\boldsymbol{l}^\kappa+\boldsymbol{x}^\kappa\|_\infty-\alpha)_+|\hat{\boldsymbol{l}}^{-\kappa}\}, \end{aligned} \quad (12)$$

where $(\cdot)_+=\max\cdot,0$. Note that, $\alpha\triangleq\|\boldsymbol{l}^{-\kappa}+\boldsymbol{x}^{-\kappa}\|_\infty$ is already known. Given the conditional distribution of the feeder load in the remaining decision horizon the optimization in (12) can now be solved in a way similar to Section III-A1.

The conditional distributions in (12), are approximated by modifying the ARMA model in (4) for the remaining horizon, so as to include only those prior days with *similar load profiles* to those observations $\hat{\boldsymbol{l}}^{-\kappa}$ in the previous time slots. We use the *cross-correlation* as a measure of similarity between the above time series [23]. At each time slot κ, we obtain the cross-correlation between $l[1],\ldots,l[\kappa]$ and the feeder load during the same time frame on a previous day [36]. We include the data points of those previous weekdays $p\in\mathcal{Q}$ over the past two weeks that have correlation higher than a minimum threshold, here set at 0.75, during the time slots $\tau=1,\cdots,\kappa$, with the load data of the operating day:

$$l[\tau]=\sum_{p\in\mathcal{Q}}a_{p,\tau}l_{-p}[\tau]+e[\tau] \qquad \forall\tau=\kappa,\cdots,\mathcal{T}. \quad (13)$$

The model coefficients in (13) are estimated similar to the offline approach. The constraints in (12) are the same as those described in Section III-A2; only here they are applied on the remaining time slots of the decision horizon. The initial SoC for the optimization at time slot κ is $C[\kappa-1]$, which was fixed at the optimization step during the previous time slot.

IV. Experimental and Numerical Results

The results in this section are presented in two categories: experimental results, and numerical results. The experimental results are inevitably bounded by two operational constraints:

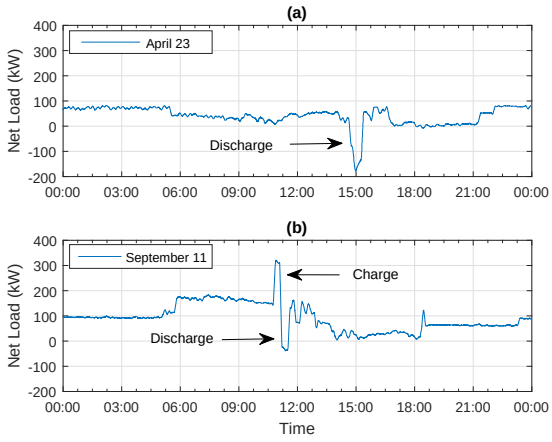

Fig. 7. Battery operation signatures at Building load on 4/23 and 9/11.

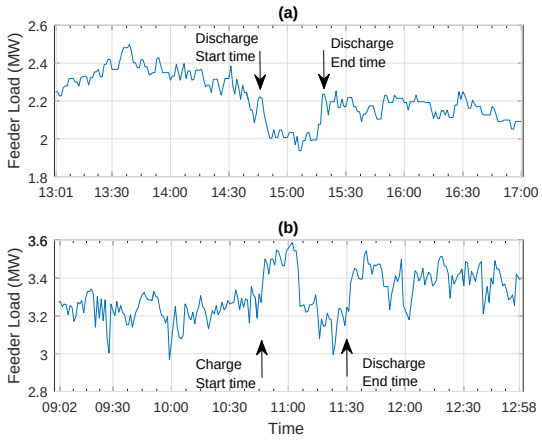

Fig. 8. Battery signatures at Feeder #1224 on 4/23 and 9/11.

1) The real-world battery system that is studied in this paper was owned by the customer and intended to help the customer lower its own electricity bill. However, based on the analysis in Section II, there is a conflict between the customer's goal and the goal of conducting feeder-level peak load reduction. Therefore, we had no choice but to do only a few number of experiments in order to minimize the financial loss that our experiments would impose to the customer on its electricity bill.
2) While the utility was able to provide the research team with reliable access to the feeder data in a minutely resolution on a daily basis, moving to the next step of providing access to the feeder data in real time was not an option due to logistical and legislative challenges. Accordingly, our experimental results are based on the offline design while our numerical results cover both the offline and online designs. Of course, even the numerical results are based on real-world feeder data and therefore they can shed light on what can be achieved, should the utility provide access to the feeder data in real time.

A. Experimental Results

To facilitate the experiments, an automated computer control system was developed that collects the utility and building data, processes it, obtains the battery schedules, and applies them through an Ethernet connection to an ARDUINO controller [37] that directly commands the inverters and the battery management system (BMS) for the two available 500 kWh / 100 kW battery units, which together form the 1 MWh / 200 kW battery system in the building microgrid. Each battery unit consists of 160 cells of 1000 Ah Li-ion Winston batteries [38], connected in series with nominal 3.2 V per cell. Each battery pack is connected to a 100 kW Princeton GTIB-100 Bi-directional inverter with a 290-800 V DC bus [39].

1) Experiments 1 and 2, Feeder Impact Experiments: These initial experiments were designed to validate system operation and control prior to the testing and evaluation of the proposed operation approach in Section III, and to test whether a substantial impact could be made on the feeder load profile. In these two experiments, the batteries are discharged and charged at full rated capacity of the inverters, i.e., about 200 kW combined, in order to examine to what extent their operation can have visible impact on the building's and feeder's load profiles. The latter was of particular interest because the building's load only constitutes a small portion of the feeder's total load. Experiment 1 was done on April 23, 2:45-3:15 PM, during which the feeder load was *relatively low*. The batteries were discharged for 30 minutes. Experiment 2 was done on September 11, 10:45-11:30 AM, during which the feeder load was *relatively high*. This time, given the higher load of the feeder, the experiment included charging of the batteries for 20 minutes, immediately followed by a discharge for 25 minutes.

Fig. 7 shows the impacts on the building's load profiles. In Fig. 7(a), the net load of the building drops by about 200 kW for a period of 30 minutes. In Fig. 7(b), the net load of the building first increases by about 180 kW, during the charge operation, and then suddenly drops by about 350 kW, once the discharge operation starts. The signatures in both experiments are clearly visible in the building's net loads.

Fig. 8 shows the impacts on the feeder's load profiles. As expected, the signatures are not as extreme as in the case of the building's net load profiles; nevertheless, the signatures in both experiments are still clearly visible. Importantly, the results of these experiments also confirm the correct operation of the developed computer control modules of the battery system.

2) Experiment 3, Feeder Peak Load Reduction Experiment: In this experiment, we implemented our proposed optimization-based design for the operation of the batteries in order to reduce the feeder's peak load. Accordingly, Experiment 3 took a whole day, on November 2. The charge and discharge schedule is decided right before mid-night on November 1. Due to the complexity of the real-world battery and charger system, the true charge and discharge round-trip efficiency is not known in advance. Thus, the batteries were assumed to have ideal efficiency, with a caveat to monitor the true efficiency from the results. This true efficiency can then be used in future operation, see Section IV-B4.

Fig. 9 shows the feeder's load profile *with* and *without* the use of batteries. Note that, only the load with the use of batteries was actually measured in this experiment; however, one can also accurately estimate the load profile without the batteries by subtracting the power consumption and power injection of batteries, which too were measured separately.

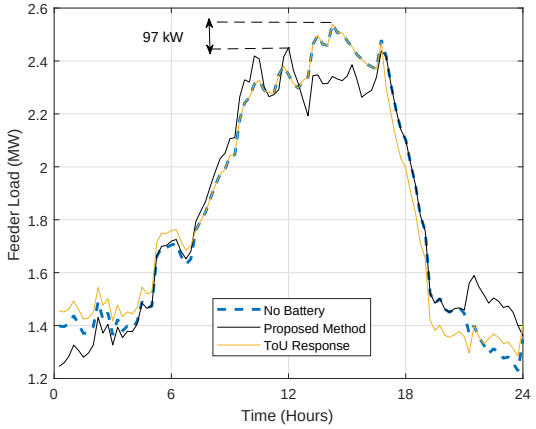

Fig. 9. Experimental result for peak feeder-load reduction on November 2.

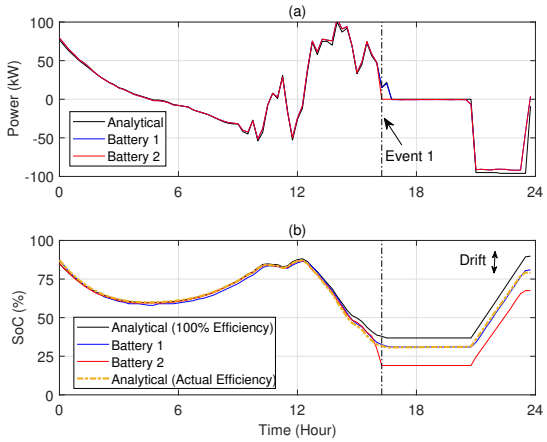

Fig. 10. Experimental results for operation of two battery modules on November 2: (a) charge and discharge powers; (b) state-of-charge.

From the results in Fig. 9, our proposed design was able to reduce the peak-load on the feeder by 97 kW, which is very promising considering the relatively small power rating of the battery inverters and also the randomness in feeder load.

The normal battery operating schedule would be to charge evenly from empty to full during the off-peak ToU hours, and discharge evenly and completely during the on-peak ToU hours. Interestingly, if the batteries operate based on the building's routine battery schedule, then *no peak load reduction* would be achieved on the feeder. This is not surprising, given the exploratory observations that we made earlier in Section II, noting that the building is discharging at the utility's system-wide peak hours which do *not* coincide with that of the feeder.

Fig. 10 shows the output of the batteries and their SoCs during Experiment 3. Here, the analytical values that are obtained from our models are compared with the values that are reported by the BMS. Next, we can make multiple interesting observations with practical importance.

First, we see that although the batteries power outputs closely follow the set points from the optimization problem with negligible delays, the values measured by the BMS at the DC link are *not* exactly the same as the set points sent to the inverters. For instance, when the batteries are charged from 9:00 PM to 11:00 PM, the power flow into the batteries is slightly *less* than the set points. In contrast, when the batteries are discharged, the power flow from the batteries is slightly *more* than the set points, which is more notable at higher inverter power outputs. This is due to the *non-ideal efficiency of inverters*. While the controllers try to follow the set points at the AC side of the inverters, the losses, though very small, deviate the power outputs of batteries from their set-points. From the results in Fig. 10(a), and also by using the charge and discharge signature data in Fig. 7, we estimated the inverter efficiency to be $\eta^d_{inv} \approx 1/\eta^c_{inv} = 0.97$ for both inverters.

Second, there is a gradually increasing difference between the experimental and analytical SoC values. This is again due to the *non-ideal efficiency* of both batteries and inverters. The energy losses from batteries' non-ideal efficiency lead the measured SoC to *slowly drift downward* from the analytical SoC throughout the day. Note that, neglecting the non-ideal battery efficiency would have a less severe impact in the online design, as the SoCs are repeatedly acquired from the BMS and the optimization solution is updated at each time slot. The impact of batteries non-ideal efficiency should be taken into account by considering appropriate charge and discharge efficiency values in both online and offline designs.

Estimating the battery efficiency accurately, can be achieved by different approaches such as in [40]. One option is approximate the values of η^c_{bat} and η^d_{bat} in (5) by minimizing the fitting error of the model and the experimental results. We used the data of both batteries during the one day experiment, assuming that both batteries have similar characteristics. Accordingly, we obtained $\eta^c_{bat} \approx 1/\eta^d_{bat} = 0.95$. Yet, these values also include the errors of BMS SoC estimation and the true efficiency may be even lower.

In Fig. 10, we can see that when these efficiency coefficients are taken into account, the SoC curve fitting is much better, barring any unforeseen events such as the SoC jump on Battery 2. The actual SoC drift can be seen in Fig. 11. When the estimated efficiency is close to the true efficiency, the maximum drift is $\leq 3\%$ at all times, while in the case where efficiency is ignored, the SoC continues to drift away from the true SoC up to almost 8%. This means that the third experiment has provided us with another operational variable that can be used to refine the model. If the true SoC were to violate the limits in an operational system, for example by sending a discharge command when the battery is empty, then the system would have no choice but to shut down for safety. However, now that the maximum drift and efficiency are known, we can, as a reliability measure, tighten the SoC limits in (7) by 3% to guarantee that the SoC drift will never impact the battery schedule. This condition of sending a discharge command when the battery is empty is exactly what causes the issues seen in Table II in Section IV-B4.

The charge and discharge battery efficiency coefficients will be used later in Section IV-B to assess the impact of considering non-ideal battery and charger efficiency on the performance of both offline and online designs.

Third, we see that the SoC for the second battery suddenly drops to $C^{\min}$ at 4 PM. Since the SoC is lowered to below $C^{\min}$, the battery stops discharging. This event can be understood by considering the BMS *errors* in estimating SoC. It is important to note that, in practice, unless the battery is

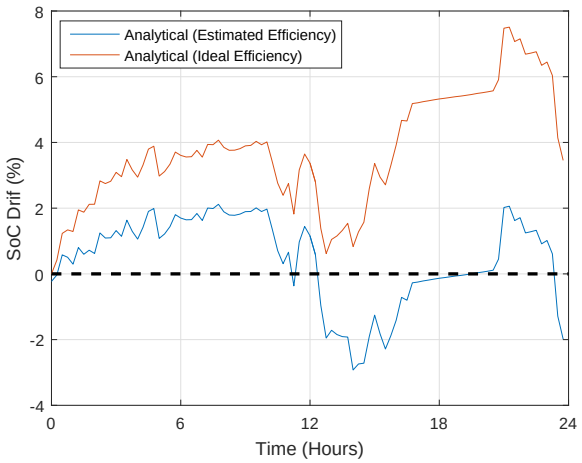

Fig. 11. Battery SoC estimation drift over time for two analytical designs, one assuming ideal efficiency and one using estimated real-world efficiency.

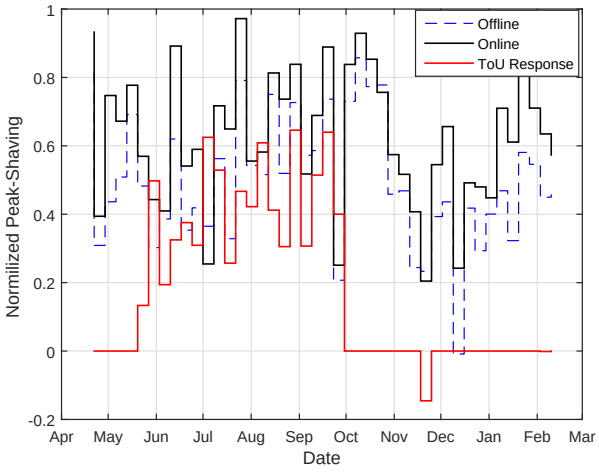

Fig. 12. The weekly normalized amount of peak load shaving achieved on the feeder by operating the battery system based on responding to ToU pricing, offline stochastic optimization, and online stochastic optimization.

fully charged or fully discharged, the SoC estimation that is made by BMS has some error. Without regular calibration, the reported SoC *drifts apart* from the actual SoC over time.

At Event 1, the true SoC was much lower than what the BMS reported,, when a battery cell triggered the BMS low limit the system recalibrated to the true SoC and the drift was corrected. Calibration can be done, e.g., by operating a full charge or a full discharge cycle. In this experiment, once the battery reaches a very low SoC, the BMS is able to *recalibrate*, suddenly realizing the error in SoC estimation, and subsequently stopping the discharge cycle.

We note that the quality of how closely the SoC levels that are calculated by the optimization follow the reported SoC values of the BMS depends on the accuracy of the parameters such as cell capacity, battery efficiency, and round-trip efficiency. In Experiment 3, in absence of knowing such parameters, the system is assumed ideal and in turn those parameters are estimated from the operation results.

B. Numerical Results

The experimental results in the previous section are promising and show how the proposed approach can reduce the peak load at distribution feeder. However, in order to make solid conclusions about the proposed schemes, one needs to conduct similar experiments for several weeks and months and for different choices of objective functions and constraints. Therefore, next, we conduct several numerical studies to further evaluate the proposed offline and online designs.

The numerical studies are performed based on utility's SCADA data on Feeder #1224 from March 2015 to February 2016. The schedules for the battery system are obtained continuously and optimally over this SCADA data.

1) Feeder Peak Load Reduction - Ideal User: This test case is aimed at assessing the maximum peak shaving performance of the two designs with respect to the feeder load uncertainty at the time of decision. Accordingly, the cost implications for the battery owner are *not* considered. That is why we refer to this test as *Ideal User*. With the same goal, for now, the batteries are assumed ideal to remove the battery inefficiency impact on performance loss in the offline and online designs.

Fig. 12 shows the results of feeder peak shaving achieved by the offline and online designs, as well as the ToU Response design. The weekly average peak reductions are normalized based on the maximum achievable values in the ideal user design. One can make several observations from this figure.

First, both offline and online stochastic designs outperform the ToU response. The performance of the online design is particularly promising as it more frequently updates its prediction of the feeder load profile during the operation. Therefore, we can conclude that there is great potential benefit to deliver an online design, as long as the logistical and legislative issues could be resolved to allow DERs, such as large batteries, to have access to feeder SCADA data.

Second, all approaches perform weaker during the Winter. This is also verified in Fig. 13, where the distributions of peak shaving achieved in offline and online designs are compared in Summer and Winter. The feeder load fluctuates more in Winter, thus, the prediction error is greater. The ToU Response is particularly poor in Winter, when no peak shaving is achieved. Recall from Section II that in Winter, the feeder peak load does not often reside in utility's peak hours.

Third, the battery system operation based on ToU Response, leads to much less feeder peak reduction, particularly in Winter when in fact *no peak shaving* is achieved. Note that, in ToU Response, the battery system does not have the objective of shaving the feeder peak load. Instead, it operates for customer internal purposes, to reduce the energy charges with respect to ToU pricing (refer to Appendix A for design formulation). Recall from Section II that in Winter, the feeder peak load does not often reside in utility's peak hours. Accordingly, while in the summer season discharging the battery in the utility peak hours might also lead to some feeder peak shaving by chance, during the winter season, discharging in those hours will not lead to any feeder peak load shaving.

Fourth, in a few instances, the performance of the proposed designs falls below the ToU response designs. These rare cases are mostly due to forecast errors or abnormalities in the feeder

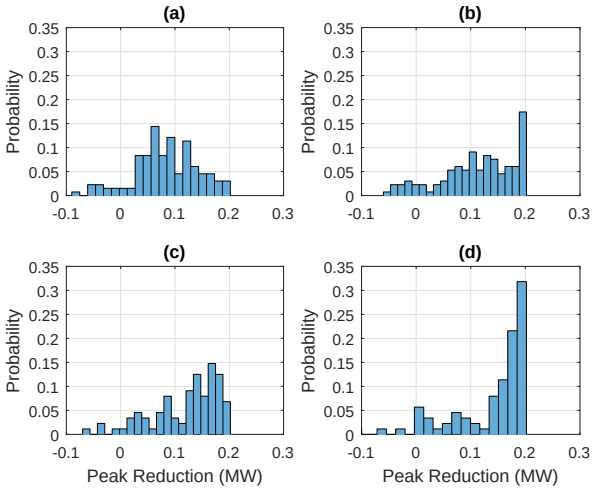

Fig. 13. The distributions of feeder peak-shaving during the two seasons from operating the battery based on: (a) Offline design in Winter, (b) Online design in Winter, (c) Offline design in Summer, (d) Online design in Summer.

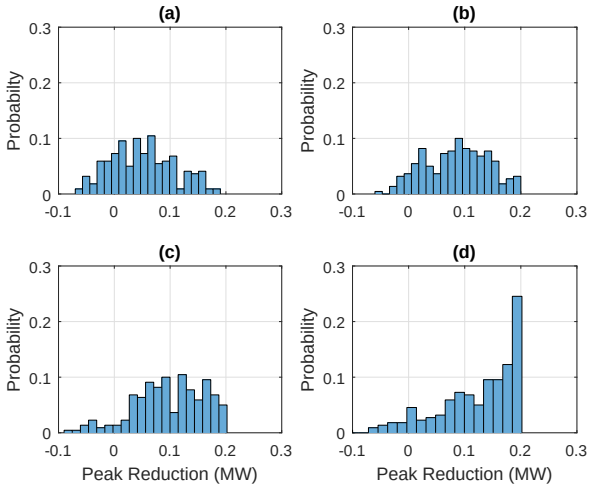

Fig. 14. The distribution of feeder peak-shaving achieved by operating the battery system over one year based on: (a) offline deterministic, (b) online deterministic, (c) offline stochastic, and (d) online stochastic designs.

TABLE I
TRADE OFF BETWEEN ENERGY COST AND PEAK SHAVING

Case No.	Average Monthly Cost ($) (Summer/Winter)	Peak Load Reduction (KW)		
		Average (Summer/Winter)	80% Confidence Interval	
			Summer	Winter
I	1861/2359	140/113	[86,200]	[28,200]
II	1496/1481	140/110	[85,200]	[27,200]
III	1831/2002	140/100	[86,200]	[15,200]
IV	1229/1436	88/0	[0,133]	[0,0]

load, e.g., during national holidays or maintenance events.

2) Performance and Cost Trade-off: From the second observation in the previous subsection, the battery operation for feeder peak load shaving may lead to extra costs under typical ToU pricing. Therefore, in this section, we assess the trade-off between the two objectives of feeder peak shaving and user's charge minimization. We evaluate the cost and performance in four cases, where the battery operates to:

1) Exclusively shave the peak load of the distribution feeder based on the online design as in Section IV-B1. This method has no regard for the customer costs.
2) Primarily shave the peak load, but with the additional objective terms related to reducing the user's charges. This is accomplished by adding a low value term to the objective that has the goal of penalizing charging during anytime besides off-peak hours, see Appendix A.
3) Primarily shave the peak load, but with additional constraints in (10) to limit peak hour charging. This design will not allow any charging during on-peak hours.
4) Exclusively reduce the user's charges based on ToU pricing, with no regard to peak load shaving. The battery simply discharges evenly during peak times and charges evenly during off peak times, see Appendix B.

The results are shown in Table I. The schedules obtained based on Case I, i.e, where the battery operation objective is to shave feeder peak load with no regards for the cost, generally lead to better performance. At the same time, in this design, the energy costs of the customer, billed by ToU pricing, are more because the battery may not lower utility peak hour loads. We also observe in Table I that in Cases II and III, by including the user cost considerations while the feeder peak shaving is still the primary objective, the customer can also utilize the batteries to reduce the energy costs. The performance loss due to extra constraints or objective terms in Cases II and III is not significant, particularly in Summer. This is consistent with our discussion in Section III. Accordingly, if for example the customer is compensated by the utility for each kW of feeder peak shaving service, the revenues of the customer for Cases II and III will be higher. Finally, the energy costs in Cases I to III, i.e. the designs that battery operates to provide feeder peak shaving service, are more than that of Case IV, i.e. the design that battery is operated only for energy cost reduction. Interestingly, the additional cost in Case II, where reducing the energy costs is secondary objective, is insignificant.

3) Method of Optimization: Next, we compare the peak-shaving performance under four different optimization approaches: offline stochastic, i.e., as in Section III-A, online stochastic, i.e., as in Section III-B, offline deterministic, i.e., when the model in (2) is used, and online deterministic. The results, in the form of the distributions of peak-shaving during one year of feeder data, are compared in Fig. 14. The performance is noticeably better for proposed stochastic optimization than the deterministic optimization in both offline (49 kW on average) and online (40 kW on average) scenarios. This confirms that the proposed stochastic optimization approaches improve feeder peak-shaving performance.

4) Impact of Battery Inefficiency: The optimization models often have errors in the estimation of the battery's available energy. The error results from multiple factors, e.g., inaccuracy of most battery models, inaccurate models parameters, and the approximations made to have a tractable optimization. This may affect the storage system performance at times, when the battery halts discharging and is forced a down-time, such as in Event 1, which is not foreseen by the controller.

The detailed analysis of the battery efficiency modeling and its impacts on storage performance is complex and still an open problem [41]. However, we can still assess the impact of inaccurate efficiency parameters within our optimization,

TABLE II
IMPACT OF BATTERY EFFICENCY MISMATCH

Assumed Efficency	Actual Efficency	Downtime (h) (Offline / Online)	Reduction (kW) (Offline / Online)
100	100	0 / 0	99 / 140
100	95	171.5 / 50.5	94.5 / 85.5
100	90	279.5 / 55.75	85 / 83.5
100	85	375 / 58.75	73.1 / 81.6
100	80	460 / 64	59.3 / 79

TABLE III
SENSITIVITY OF FEEDER PEAK LOAD REDUCTION TO EFFICIENCY

Efficiency	Average Daily Reduction (kW)
100	128
95	124
90	118
85	112
80	105

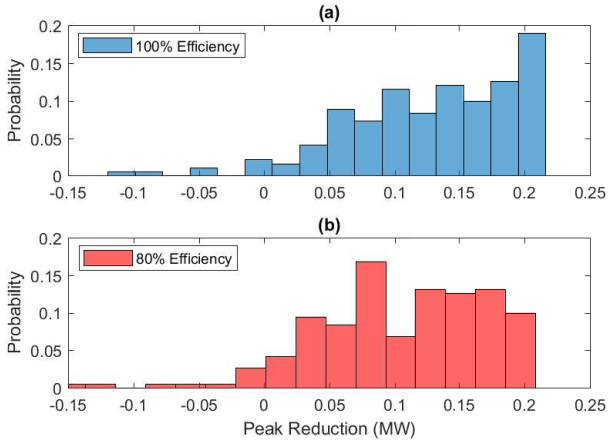

Fig. 15. Impact of ignoring or considering system efficiency in the design optimization on the distribution of the amount of feeder peak load shaved for a complete year (a) 100% efficiency (ideal) and (b) 80% efficiency.

on the overall performance of the offline and online designs. Note that, with respect to efficiency, the two designs have a difference in how frequently they update the SoC estimates from the BMS reported values. We assume that the SoC values are obtained from (5), given the efficiency parameters, and based on the schedules set in each design, prior to each operation horizon. The true SoC at the end of each horizon is then given as inputs for C^0 in the next round of optimization. Additionally, the down-time periods are calculated by the evaluation simulation, after the optimization schedules are set for each time horizon in both designs.

Table II shows the results of *down-time hours* and *peak-shaving loss* due to battery inefficiency for both offline and online designs. We can see that, the impact of efficiency mismatch on the down-time hours caused by discharging the battery when it is already depleted is particularly notable in the offline design. As the SoC estimation error *accumulates* over time, so do the events that lead to storage downtime. Although, not all of such events affect the peak-shaving performance. In fact, ultimately, the average peak-shaving is reduced considerably during one year of battery operation.

An interesting observation is that the online design performance is also very sensitive to the estimation error in the battery's SoC. While the total downtime duration due to such errors is much less than the offline design, the peak reduction is severely affected by the few instances the battery halt discharge in a required period. This further raise attention to the SoC estimation error impact, which may not be neglected even with frequent updates from the measured values.

We can see from Table II that the feeder peak load reduction is significantly impacted by efficiency mismatch, therefore, it is important that one does not assume ideal efficiency in practical hardware operation. This leads to a need to model and further study the impact of system efficiency. Therefore, we use an experiment similar to Experiment 3 in Section IV-A2 to estimate the charge and discharge efficiency and then use these numbers to assess the impact on peak load reduction. Table III shows the effect of efficiency on peak reduction. When the optimization considers the efficiency the results are much better than those shown in Table II. The efficiency also has an impact on the peak reduction distributions. Fig. 15 shows the distribution for 100%, and 80% efficiency. Even though the potential maximum reduction is the same, the lowered efficiency begins to have a substantial impact on the distribution. However, this impact is still less than if the battery efficiency is estimated incorrectly, so a proper estimate is vital.

V. CONCLUSIONS

It was shown that the feeder peak load and the utility-wide peak hours may not be aligned, confirming the need for a localized solution with proper utility-resource communications for feeder-level peak load reduction. A stochastic optimization-based framework was developed and implemented, to demonstrate conducting peak load reduction at a distribution feeder using customer owned batteries, under both offline and online control settings. The feeder load uncertainty was addressed under both designs and was shown that the auto-regressive nature of the load, observed in historical data, may be leveraged to achieve effective performance. Multiple experimental tests were performed by operating a 1 MWh / 200 kW battery at a commercial building. They verified the considerable reduction of the feeder peak load achieved based on the proposed framework. They also showed many operational issues that may not be foreseen in computer simulations, such as the need to carefully calibrate BMS state-of-charge estimates and to take into account operational efficiency/SoC drift. Additionally, various numerical assessments was performed based upon one year of real-world feeder data, that allowed further evaluations of the proposed design as well as practical observations.

REFERENCES

[1] J. Ye, J. Xue, B. Sang, D. Lu, and H. Liu, "Economic value and government compensation calculative method of energy storage system," in *2016 IEEE 8th International Power Electronics and Motion Control Conference (IPEMC-ECCE Asia)*, May 2016, pp. 536–540.

[2] T. Feehally, A. J. Forsyth, R. Todd, M. P. Foster, D. Gladwin, D. A. Stone, and D. Strickland, "Battery energy storage systems for the electricity grid: UK research facilities," in *8th IET International Conference on Power Electronics, Machines and Drives (PEMD 2016)*, April 2016.

[3] "http://www.energy.ca.gov/electricity–analysis/rule21."

[4] A. Shahsavari, A. Sadeghi-Mobarakeh, E. Stewart, E. Cortez, L. Alvarez, F. Megala, and H. Mohsenian-Rad, "Distribution grid reliability versus regulation market efficiency: An analysis based on micro-pmu data," *IEEE Trans. on Smart Grid*, vol. PP, no. 99, pp. 1–10, 2017.

[5] A. Shahsavari, M. Farajollahi, E. Stewart, A. Van-Meier, L. Alvarez, E. Cortez, and H. Mohsenian-Rad, "Data-driven analysis of capacitor bank operation at a distribution feeder using micro-pmu data," in *Proc. of IEEE PES ISGT*, Washington, DC, Apr. 2017.

[6] A. Shahsavari, M. Farajollahi, E. Stewart, C. Roberts, F. Megala, L. Alvarez, E. Cortez, and H. Mohsenian-Rad, "Autopsy on active distribution networks: A data-driven fault analysis using micro-pmu data," in *Proc. of IEEE PES North American Power Symposium*, Morgantown, WV, Sep. 2017.

[7] A. Shahsavari, M. Farajollahi, E. Stewart, C. Roberts, and H. Mohsenian-Rad, "A data-driven analysis of lightning-initiated contingencies at a distribution grid with a pv farm using micro-pmu data," in *Proc. of IEEE PES North American Power Symposium*, Morgantown, WV, Sep. 2017.

[8] A. Shahsavari, A. Sadeghi-Mobarakeh, E. Stewart, and H. Mohsenian-Rad, "Distribution grid reliability analysis considering regulation down load resources by micro-pmu data," in *Proc. of IEEE International Conference on Smart Grid Communications*, Sydney, Australia, Nov.

[9] S. Chouhan, D. Tiwari, H. Inan, S. K. Solanki, and A. Feliachi, "DER optimization to determine optimum BESS charge/discharge schedule using LP," in *Proc. of IEEE PES General Meeting*, July 2016.

[10] M. Alam, K. Muttaqi, and D. Sutanto, "A controllable local peak-shaving strategy for effective utilization of PEV battery capacity for distribution network support," *IEEE Trans. on Industry Applications*, vol. 51, no. 3, pp. 2030–2037, 2015.

[11] B. Asghari, A. Hooshmand, and R. Sharma, "A service-based approach toward management of grid-tied microgrids," in *Proc. of IEEE PES Innovative Smart Grid Technologies Latin America*, Oct 2015.

[12] H. Sugihara, K. Yokoyama, O. Saeki, K. Tsuji, and T. Funaki, "Economic and efficient voltage management using customer-owned energy storage systems in a distribution network with high penetration of photovoltaic systems," *IEEE Trans. on Power Systems*, vol. 28, no. 1, pp. 102–111, 2013.

[13] C. Tan, T. Green, and C. Hernandez-Aramburo, "A stochastic simulation of battery sizing for demand shifting and uninterruptible power supply facility," in *Proc. of IEEE Power Electronics Specialists*, June 2007.

[14] C. Venu, Y. Riffonneau, S. Bacha, and Y. Baghzouz, "Battery storage system sizing in distribution feeders with distributed photovoltaic systems," in *Proc. of IEEE Bucharest PowerTech*, June 2009.

[15] H. Elsayed, S. Chaudhry, and A. Al-Mahmoud, "PV, battery storage and energy conversion system for meeting peak load in a substation," in *Proc. of CIRED Workshop*, May 2012.

[16] M. Peskin, P. Powell, and E. Hall, "Conservation voltage reduction with feedback from advanced metering infrastructure," in *Proc. of IEEE PES T&D 2012*, May 2012.

[17] X. Dong, Z. Wu, Z. Liu, H. Ji, Z. Wang, and P. Li, "Research and application on operation and control technologies of smart distribution network," in *Proc. of China Int. Conf. on Elec. Distribution*, Aug 2016.

[18] S. Abdelrazek and S. Kamalasadan, "Integrated PV capacity firming and energy time shift battery energy storage management using energy-oriented optimization," *IEEE Trans. on Industry Applications*, vol. 52, no. 3, pp. 2607–2617, May 2016.

[19] Z. Taylor, H. Akhavan-Hejazi, E. Cortez, L. Alvarez, S. Ula, M. Barth, and H. Mohsenian-Rad, "Battery-assisted distribution feeder peak load reduction: Stochastic optimization and utility-scale implementation," in *Proc. of IEEE PES General Meeting*, July 2016.

[20] K. Marti, *Stochastic optimization methods*. Springer, 2005.

[21] J. Birge and F. Louveaux, *Introduction to stochastic programming*. Springer Science & Business Media, 2011.

[22] S. Boyd and L. Vandenberghe, *Convex Optimization*. Cambridge University Press, 2004.

[23] P. Stoica and M. Randolph, *Spectral Analysis of Signals*. Pearson Prentice Hall Upper Saddle River, NJ, 2005.

[24] P. J. Brockwell and R. A. Davis, *Time Series: Theory and Methods*, 2nd ed. New York: Springer, 2009.

[25] H. Hahn, S. Meyer-Nieberg, and S. Pickl, "Electric load forecasting methods: Tools for decision making," *European Journal of Operational Research*, vol. 199, no. 3, pp. 902 – 907, 2009.

[26] H. Akhavan-Hejazi and H. Mohsenian-Rad, "Energy storage planning in active distribution grids: A chance-constrained optimization with non-parametric probability functions," *IEEE Trans. on Smart Grid*, vol. PP, no. 99, pp. 1–12, 2017.

[27] P. J. Brockwell, R. Dahlhaus, and A. Trindade, *Modified Burg Algorithms for Multivariate Subset Autoregression*. Statistica Sinica, 2005.

[28] R. H. Shumway and D. S. Stoffer, *Time Series Analysis and its Applications*, 3rd ed. Springer, 2011.

[29] S. Theodoridis, *Probability & Stochastic Processes*, ser. Machine Learning: A Bayesian and Optimization Perspective. Academic Press, 2015.

[30] H. Niederreiter, "Random number generation and quasi-monte carlo methods," *SIAM Philadelphia*, 1992.

[31] T. Koyasu, K. Yukita, K. Ichiyanagi, M. Minowa, M. Yoda, and K. Hirose, "Forecasting variation of solar radiation and movement of cloud by sky image data," in *2016 IEEE International Conference on Renewable Energy Research and Applications (ICRERA)*, Nov 2016.

[32] Y. Najera, D. R. Reed, and W. M. Grady, "Image processing methods for predicting the time of cloud shadow arrivals to photovoltaic systems," in *2011 37th IEEE Photovoltaic Specialists Conference*, June 2011.

[33] W. F. Holmgren, A. T. Lorenzo, M. Leuthold, C. K. Kim, A. D. Cronin, and E. A. Betterton, "An operational, real-time forecasting system for 250 mw of pv power using nwp, satellite, and dg production data," in *2014 IEEE 40th Photovoltaic Specialist Conference (PVSC)*, June 2014.

[34] H. Akhavan-Hejazi and H. Mohsenian-Rad, "Optimal operation of independent storage systems in energy and reserve markets with high wind penetration," *IEEE Trans. on Smart Grid*, vol. 5, no. 2, 2014.

[35] H. Akhavan-Hejazi, B. Asghari, and R. Sharma, "A joint bidding and operation strategy for battery storage in multi-temporal energy markets," in *Proc. of IEEE Innovative Smart Grid Technologies Conference*, 2015.

[36] M. Kendall, *Advanced Theory of Statistics*, 4th ed. Macmillan, 1979.

[37] "http://www.arduino.org/products/boards."

[38] "http://en.winston-battery.com."

[39] "http://www.princetonpower.com."

[40] K. Li and K. Tseng, "Energy efficiency of lithium-ion battery used as energy storage devices in micro-grid," in *in Proc. of IEEE Industrial Electronics Society Conference*, Nov 2015.

[41] A. S. Akyurek and T. S. Rosing, "Optimal distributed nonlinear battery control," *IEEE Journal of Emerging and Selected Topics in Power Electronics*, vol. PP, no. 99, pp. 1–1, 2016.

[42] R. T. Marler and J. S. Arora, "Survey of multi-objective optimization methods for engineering," *Structural and multidisciplinary optimization*, vol. 26, no. 6, pp. 369–395, 2004.

APPENDIX A
MULTIOBJECTIVE OPTIMIZATION

Due to the use of $\max$ function in the objective function in (1), there are infinite solutions to this optimization problem. Therefore, within the solution space of problem (1), we can further narrow down to the solutions that result in the highest reduction also in the customer's own utility bill. The feeder peak-shaving service is regarded as *primary* objective, while reducing the customer bill at the same time is the *secondary* objective. The properties of this problem allow us to utilize the optimization with ordered objectives. A simple approach to formulate the problem is to utilize the weight coefficients for combining both objectives into a single one as follows [42]:

$$\mathbb{E}\{\|\boldsymbol{l}+\boldsymbol{x}\|_\infty\} + \epsilon_1 \sum_{\tau \in \text{On-Peak}} x[\tau] + \epsilon_2 \sum_{\tau \in \text{Mid-Peak}} x[\tau] + \epsilon_3 \sum_{\tau \in \text{Off-Peak}} x[\tau],$$

where the weight coefficients ϵ_1, ϵ_2, and ϵ_3 are chosen to reflect the cost difference of energy during peak, mid-peak, and off-peak time periods. However, note that, these coefficients must be small enough such that they do not cause any significant change in feeder peak load reduction, i.e., they do not jeopardize the primary objective. Thus, the objective will lead to the solutions that have the same feeder load reduction, yet lead to more utility bill reduction for the customer.

APPENDIX B
CUSTOMER OBJECTIVE ONLY OPTIMIZATION

If the customer that owns the batteries were to entirely ignore the feeder and rather solely consider ToU price reduction as its operation optimization objective, then it would use Algorithm 1. This would result in full and even battery charges during the off-peak hours, inactivity during mid-peak hours, and full battery discharges during the on-peak hours.

Algorithm 1 ToU Operation

$t \leftarrow$ current timeslot
if $t \in$ On-Peak Hours **then**
  $x \leftarrow -(C_{max} - C_{min})$/Total On-Peak Hours
else if $t \in$ Off-Peak Hours **then**
  $x \leftarrow (C_{max} - C_{min})$/Total Off-Peak Hours
else if $t \in$ Mid-Peak Hours **then**
  $x \leftarrow 0$
end if

Zachariah Taylor (S'13) received the B.Sc. degree in electrical and computer engineering from California Baptist University, Riverside, CA, USA in 2013 and received the M.Sc. degree in electrical engineering from the University of California, Riverside, CA, in 2014. He is currently pursuing the Ph.D. degree in electrical engineering with the University of California, Riverside, CA, USA. His research interests include distributed resource optimization in electric power systems and operation, management, and modeling of energy storage systems.

Hossein Akhavan-Hejazi (S'12-M'17) received the M.Sc. degree in electrical engineering from Amirkabir University of Technology, Tehran, Iran, in 2011 and the Ph.D. degree in electrical engineering from the University of California, Riverside, USA, in 2016. His research interests include optimization and stochastic analysis in electric power systems, power system operations and market analysis, operation management and modeling of energy storage systems, and big data applications in power systems.

Mr. Cortez manages a staff of over 20 employees in the Communications, System Planning, Substation Engineering and Protection groups at Riverside Public Utilities. The group is responsible for the deployment and integration of electric systems to support the business processes related with advanced grid technologies and system reliability.

Lilliana Alvarez earned her Bachelors Degree in Electrical Engineering from California State Polytechnic University, Pomona in 2012. She began her career at Riverside Public Utilities as an intern in August 2012 and was promoted to Utilities Associate Electrical Engineer in 2013. Lilliana now holds the position of Utilities Electrical Engineer within the Electric System Planning Department. Lillianas experience includes transmission and distribution planning, project management, underground cable modeling, and power quality.

Sadrul Ula is the Managing Director of Winston Chung Global Energy Center, a new research center at the University of California Riverside, Bourns College of Engineering. He is also a Research Faculty at the College of Engineering Center for Environmental Research and Technology (CE-CERT) and part of the Southern California Research Initiative for Solar Energy (SC-RISE). He is working on research, development and outreach aspects of electrical energy storage, power transmission and distribution, smart grids, solar photo-voltaic (PV), solar thermal, concentrated PV (CPV) and concentrated solar (CSP), as well as wind energy.

Matthew Barth (M'90-SM'00-Fellow'14) is the Yeager Families Professor at the College of Engineering, University of California-Riverside. He is part of the intelligent systems faculty in Electrical and Computer Engineering and is also serving as the Director for the Center for Environmental Research and Technology (CE-CERT), UCRs largest multi-disciplinary research center. He received his B.S. degree in Electrical Engineering/Computer Science from the University of Colorado in 1984, and M.S. (1985) and Ph.D. (1990) degrees in Electrical and Computer Engineering from the University of California, Santa Barbara. Dr. Barth joined the University of California-Riverside in 1991, conducting research in Intelligent Systems. Dr. Barths research focuses on applying engineering system concepts and automation technology to Transportation Systems, and in particular how it relates to energy and air quality issues. Dr. Barth has also been active an associate editor of the Transactions of Intelligent Transportation Systems, and member of the IEEE ITSS Board of Governors. He was the IEEE ITSS Vice President for Conferences from 2011-2012, President-Elect for 2013, President for 2014-2015, Past President for 2016, and Vice President of Finances for 2017-2018. He recently received the IEEE ITSS Outstanding Research Award.

Hamed Mohsenian-Rad (S'04-M'09-SM'14) received the Ph.D. degree in electrical and computer engineering from the University of British Columbia Vancouver, BC, Canada, in 2008. He is currently an Associate Professor of electrical engineering at the University of California, Riverside, CA, USA. His research interests include modeling, data analytics, and optimization of power systems and smart grids. He received the National Science Foundation CAREER Award 2012, the Best Paper Award from the IEEE Power and Energy Society General Meeting 2013, and the Best Paper Award from the IEEE Conference on Smart Grid Communications 2012. He serves as an Editor for the IEEE TRANSACTIONS ON SMART GRID and the IEEE POWER ENGINEERING LETTERS.